CARBON letters

Original Articles
Carbon Letters Vol. 22, 81-88 (2017)

Extraction and characterization of lignin from black liquor and preparation of biomass-based activated carbon therefrom

Daeyeon Kim[1], Jinsil Cheon[1], Jeonghoon Kim[1], Daekyun Hwang[1], Ikpyo Hong[2], Oh Hyeong Kwon[1], Won Ho Park[3] and Donghwan Cho[1,♠]

[1]Department of Polymer Science and Engineering, Kumoh National Institute of Technology, Gumi 39177, Korea
[2]Carbon Materials Research Group, New Materials and Component Research Center, Research Institute of Industrial Science and Technology, Pohang 37673, Korea
[3]Department of Organic Materials Engineering, Chungnam National University, Daejeon 34134, Korea

Article Info
Received 10 October 2016
Accepted 30 March 2017

♠Corresponding Author
E-mail: dcho@kumoh.ac.kr
Tel: +82-54-478-7688

Open Access
DOI: http://dx.doi.org/10.5714/CL.2017.22.081

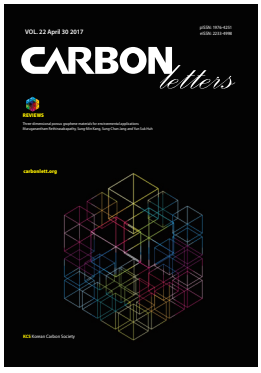

http://carbonlett.org

pISSN: 1976-4251
eISSN: 2233-4998

Abstract

In the present study, biomass-based lignin was extracted from industrial waste black liquor and the extracted lignin was characterized by means of attenuated total reflectance-Fourier transform infrared spectroscopy and ^{1}H-nuclear magnetic resonance spectroscopy. The extracted lignin was carbonized at different temperatures and then activated with steam at 850°C. The extracted lignin in powder state was transformed into a bulky carbonized lignin due to possible fusion between the lignin particles occurring upon carbonization. The carbonized and then pulverized lignin exhibits brittle surfaces, the increased thermal stability, and the carbon assay with increasing the carbonization temperature. The scanning electron microscopic images and the Brunauer-Emmett-Teller result indicate that the steam-activated carbon has the specific surface area of 1718 m^2/g, which is markedly greater than the carbonized lignin. This study reveals that biomass-based activated carbon with highly porous structure can be produced from costless black liquor via steam-activation process.

Key words: black liquor, lignin, activated carbon, steam-activation, specific surface area

1. Introduction

Recently, reuse of biomass-based industrial waste has been significantly considered as bioresource owing to increasing issues on energy saving and cost-effectiveness with social consciousness and regulation. Lignin, which can be derived from industrial waste black liquor, is one of the considerable materials as biomass-based resource. A large volume of black liquor can be obtained from chemical pulping process. It is known that black liquor of approximately 7 tons is produced as by-product in the manufacturing process of 1 ton of pulp [1]. It may be landfilled after chemical treatment or may be utilized as an energy source by combustion or gasification process [2,3]. Black liquor is aqueous solution including lignin residues, hemicellulose, and other organic chemicals (for instance, Na_2CO_3, Na_2SO_4, NaOH, and Na_2S) used in the pulping and cooking processes [4]. It is strongly alkaline with the pH value of 13. It has normally a black color and smells disgusting. The chemical composition more or less depends on the wood type and the processing condition used in the chemical pulping process [5]. In general, black liquor contains about 25–35% lignin by weight [6,7]. Lignin can be extracted in powder state from black liquor by appropriate chemical treatment and filtering process [8]. Studies on

the lignin extracted from black liquor, depending on wood type, extraction method, and pulping process, have been reported earlier [9-12].

The lignin extracted from black liquor consists of many aromatic rings in the chemical structure. The chemical structure is complicated and can often be identified by the presence of polypropane units such as *p*-hydroxyphenyl (or *p*-coumaryl alcohol), guaiacyl (or coniferyl alcohol), and syringyl (or sinapyl alcohol). The polypropane units can be chemically bonded in different bonding patterns [8,13-15]. Accordingly, its high aromaticity gives rise to relatively high thermal stability and carbon yield, being considered as a potential candidate as biomass-based carbon materials.

Carbonization process has been traditionally utilized to transform organic materials to carbonized materials with high carbon assay by pyrolysis, and ultimately to manufacture charcoal, cokes, activated carbon, carbon fiber, etc. [16-18]. Activation process has been conventionally utilized to make a non-porous or less-porous material highly porous with high specific surface area by using chemicals or gases. There are two main approaches to prepare activated carbon, physical activation using steam, carbon dioxide, oxygen, mixed gases, etc., and chemical activation using KOH, Na_2CO_3, NaOH, etc. [19-21]. Each modification method has its advantages and disadvantages. It has been known that the physical activation method is environmentally friendly, whereas the chemical activation method is relatively effective [22].

Activated carbon is a highly porous material having the specific surface area greater than 1000 m^2/g with a huge number of micropores and/or mesopores, in general [23]. The characteristics of activated carbon depend on the precursor material and the processing parameters used in carbonization and activation processes. As a result, the absorption-desorption behavior may be influenced as well. At present, commercial general-purpose activated carbon has been widely produced from coconut shells, saw dusts, wood, pitch, bituminous coal, etc. [24,25]. Brunauer-Emmett-Teller (BET) analysis is most widely used to measure the specific surface area of activated carbon and to understand the micropore formation with assistance of scanning electron microscopic images [26,27]. Isotherm adsorption-desorption behavior also provides useful information on the physical adsorption of a gas of interest and the pore structure of activated carbon [28-30].

There have been a number of papers on carbonization [17,28,31] and activation [20,32,33] of biomass-based natural resources including natural fiber, wood, etc. However, studies on the activated carbon prepared from black liquor have been scarcely found.

Consequently, the objective of the present study is to extract biomass-based lignin from industrial waste black liquor, to characterize the extracted lignin, and ultimately to investigate the feasibility of producing black liquor-derived activated carbon. As a preliminary study, carbonization and steam-activation processes are performed and the obtained activated carbon is characterized in terms of thermal stability, X-ray diffraction pattern, morphology, and specific surface area.

2. Experimental

2.1. Raw materials

Black liquor used in the present work is a biomass-based industrial waste obtained from the chemical kraft pulping process of wood. It was kindly supplied from Moolim P&P Co. Ltd. (Korea) and used to extract lignin therein throughout a series of experimental procedures. Sulfuric acid of 95% purity, which was purchased from Junsei Co. (Japan) was used to lower the pH value of black liquor during the extraction process.

2.2. Lignin extraction

The 'as-supplied' black liquor exhibits the pH value of about 13. In order to extract the lignin component therein, dilute sulfuric acid (4 M, 22% by weight) was added in the black liquor and then agitated using a magnetic stirrer until the pH value decreased to 2. The pH value of 2 is for obtaining the increased yield of the extracted lignin, as reported earlier [11]. At this time, the color of black liquor turned from black to brown, resulting in some precipitate. After additional agitation of the precipitate for 1 h, the pH value of the precipitate was controlled to be about 5–6 with distilled water by using suction-filtering equipment. The obtained product was dried at 45°C for 36 h in a vacuum oven and then finely pulverized using a mortar. Without additional purification procedure, the pulverized product was tightly sealed and kept at ambient temperature prior to use.

2.3. Carbonization and activation processes of extracted lignin

Carbonization processes were carried out at 600, 850, and 1000°C with the heating rate of 1°C/min using a tube-type Siliconit carbonization furnace (Ajeon Co., Korea), respectively. The inner diameter of the tube furnace is 80 mm and the length is 1000 mm. The heating zone in the middle of the furnace is 200 mm. The both ends of the furnace were designed to control the inlet and outlet of a purging inert gas. The pulverized lignin was put in an alumina crucible on a rectangular-shaped graphite plate (2500 mm×60 mm×10 mm) and then the plate was gently placed in the center of the heating zone. The carbonization was performed purging a nitrogen gas (99.9%) throughout the process.

Activation process was carried out in the presence of steam with a purging nitrogen gas by using a tailor-made tube-type activation furnace. The tube dimensions of activation furnace are similar to those of carbonization furnace. The carbonized lignin was put in an alumina crucible on the graphite plate and then the plate was gently placed in the center of the heating zone.

The heating rate of 1°C/min was used up to 850°C and then steam was supplied at 850°C for 1 h without purging a nitrogen gas, as informed earlier [34]. Water was supplied with the rate of 3 mL/min to a steam generator (TC200P; MTOPS, Korea) pre-set to 200°C and then the generated steam was uniformly supplied to the carbonized lignin through a steam-tube line by using a quantifying pump (Masterflex MODEL NO. 7524-05; Cole-Parmer Instrument Co., Korea).

Table 1. Processing parameters for carbonization and steam-activation processes used in this work

Processing parameter	Carbonization	Steam-activation
Temperature (°C)	600, 850, 1000	850
Heating rate (°C/min)	1	1
Holding time (min)	-	60
Steam injection (mL/min)	-	3
Atmosphere	N_2 (99.9%)	N_2 (99.9%)
Gas flow rate (mL/min)	150	150
Cooling	Natural cooling	Natural cooling

In both carbonization and steam-activation processes, heat-treatment temperature, heating rate, heating step, and dwell-time were changeable by using the controller. Table 1 summarizes the processing parameters for the carbonization and steam-activation processes used in this work.

2.4. Characterization

The weight changes occurring during the carbonization and steam-activation processes were measured by using an analytical balance. The surfaces of the extracted and carbonized lignin materials were observed by using a scanning electron microscope (SEM; JSM-6380, JEOL, Japan). The surfaces of the activated carbon were observed by means of field emission-SEM (FE-SEM; JSM-6701F, JEOL, Japan). All samples for SEM observations were uniformly coated with platinum for 3 min by a sputtering method.

The thermal stability of the extracted and carbonized lignin samples was measured to 800°C in a nitrogen atmosphere by means of thermogravimetric analysis (TGA; Q500, TA Instruments, USA). Each sample of about 20 mg was placed in a platinum pan. The heating rate was 10°C/min.

^{1}H-Nuclear magnetic resonance spectroscopy (AVANCE III 400; Bruker Biospin, Switzerland) was used to explore the chemical structure of the extracted lignin. Dimethyl sulfoxide-d_6 (DMSO-d_6) was used as solvent of lignin. In order to investigate the chemical functional groups existing in the extracted lignin, attenuated total reflectance-Fourier transform infrared spectroscopy (ATR-FTIR; Nicolet 6700 FT-IR Spectrometer, Thermo Fisher Scientific Inc., UK) was also used. The crystal material for ATR-FTIR analysis was zinc selenide.

The X-ray diffraction analysis of the extracted and carbonized lignin samples was performed by means of a high resolution Xray diffractometer (D/MAY-2500/PC; Rigaku, Japan). The 2θ range for scanning was 2–60°. The targeting radiation was K_α and the targeting material was Cu.

An elemental analyzer (Flash 2000; Thermo Fisher, UK) was used to examine the chemical compositions (C, H, and N) of the extracted and carbonized lignin samples. The oxygen content was estimated by subtracting the C, H, and N contents from the total.

A surface area and pore size analyzer (ASAP2020; Micromeritics Inc., USA) was used to investigate the specific surface area and the pore characteristic of the activated carbon. The specific surface areas of the carbonized lignin and the activated carbon were measured. Prior to the measurement, each sample was evacuated at 300°C for 10 h. Isotherm-adsorption and desorption curves of N_2 at 77 K were also obtained. The specific surface area, micropore area, and external surface area were calculated by using the following equation [35].

$$A_s=(m/22414)t_m N_a \sigma,$$

where t is the statistical thickness of the adsorbed layer, m the slope of the t-plot (adsorbed volume against t), which is directly proportional to the surface area A_s, the N_a the Avogadro number, and σ the area covered by one nitrogen molecule. The external surface area was calculated by subtracting the micropore surface from the specific surface area.

3. Results and Discussion

3.1. Chemical structure of the extracted lignin

Fig. 1a shows the ATR-FTIR spectrum of the extracted lignin. The enlarged spectrum between 1800 and 700 cm^{-1} is

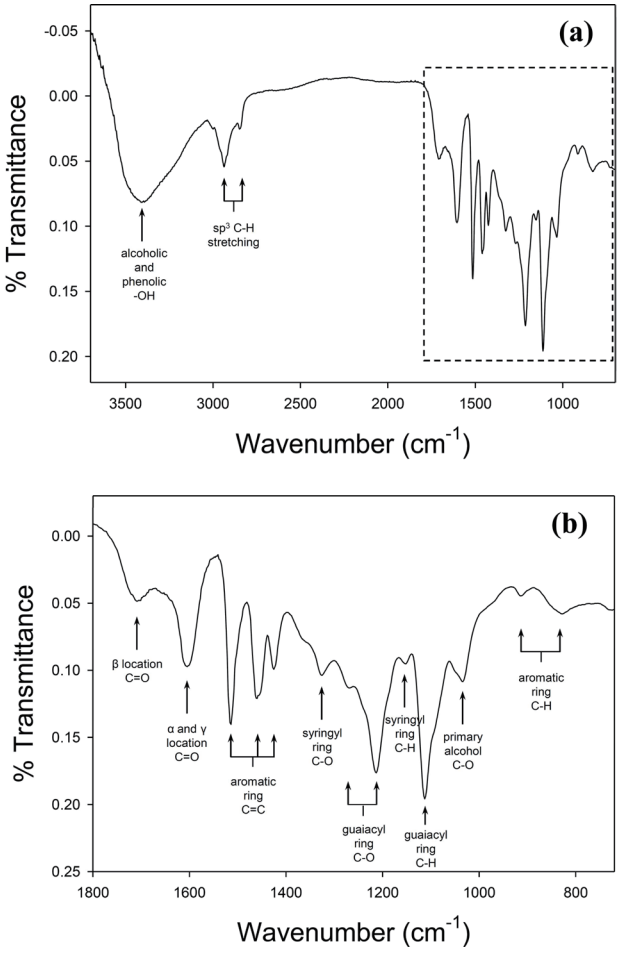

Fig. 1. Attenuated total reflectance-Fourier transform infrared spectroscopy absorption spectra (a) measured with the extracted lignin and the absorption spectra (b) between 1800 and 700 cm^{-1}.

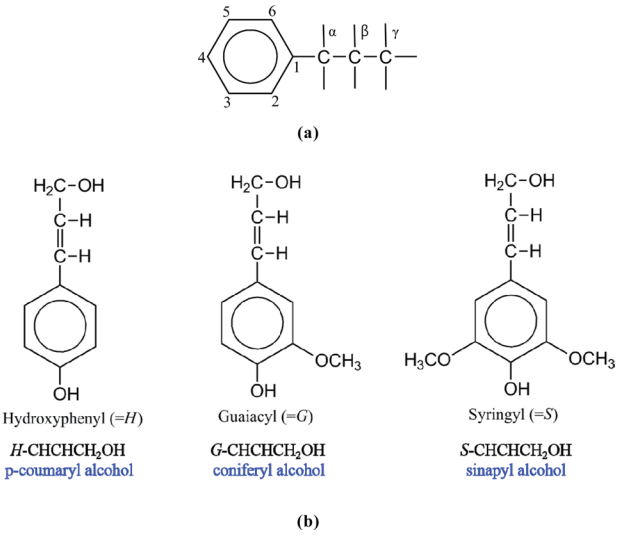

Fig. 2. Chemical structures of lignin constituents: (a) base structure of phenylpropane unit and (b) the major chemical components constituting of lignin [37].

shown with the assigned chemical groups in Fig. 1b. From Fig. 1a, the relatively large and broad absorption peak is due to hydroxyl groups in the alcohol and phenol moieties existing in the lignin. The small peaks at 2936 and 2842 cm^{-1} are due to sp^3 C-H stretching. It is confirmed that the absorption peaks at 1715 and 1603 cm^{-1} are carbonyl peaks existing in the β position and also in the α and γ positions of phenylpropane unit, respectively, as found earlier [12]. The existence of C-O group owing to the primary alcohol is also found from the peak near 1032 cm^{-1}. The peaks at 1500 and 850 cm^{-1} indicate the presence of aromatic C=C and C-C groups, respectively. Importantly, the peaks at 1313 and 1111 cm^{-1} indicate the C-O and C-H groups in the syringyl ring and the peaks near 1220 and 1810 cm^{-1} reveal the C-O and C-H groups in the guaiacyl ring. It has often been found that the presence of the syringyl and guaiacyl rings is from hardwood [36]. It has been informed by the manufacturer that the black liquor used here was originated from the by-products of pulping process using hardwood. The ATR-FTIR result demonstrates that biomass-based lignin was successfully extracted from 'as-supplied' black liquor. Fig. 2 shows the chemical structure of lignin constituents with the base phenylpropane unit (a) and the main chemical components (b), as characterized here and also as reported in other literature [37].

Fig. 3 displays ^{1}HNMR spectrum of the extracted lignin. The peak at 2.50 ppm is due to DMSO-d_6 used as solvent. The peak at about 3.40 ppm is due to hydrogen of H_2O in the solvent. The small peak at 1.23 ppm indicates the presence of hydrogen in the aliphatic group of lignin. The peak at 2.18 ppm is due to the -CH- hydrogen in CH_2OH group. The strong peak due to hydrogen in the methoxy group is found at 3.51 ppm. The peak at 3.76 ppm is ascribed to the -CH_2- hydrogen attached to the -COO- group. The peak at about 4.20 ppm is explained by hydrogen in the -HC-O-CH_2- moiety bonded by an ether linkage. Importantly, the existence of hydrogen in the aromatic groups of the lignin structure is elucidated from the peaks in the range of 6.5–7.5 ppm, as found earlier [38].

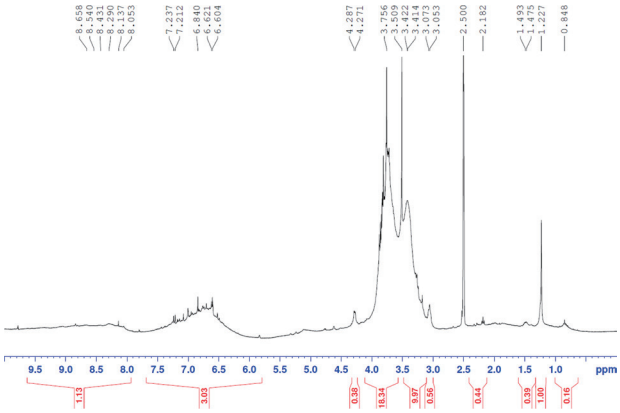

Fig. 3. ^{1}H-nuclear magnetic resonance spectroscopy spectrum measured with the extracted lignin.

3.2. Yield and appearance of the extracted lignin and carbonized lignin

Black liquor of about 100 g was used in every extraction procedure described earlier. The extraction yield of lignin from the black liquor was about 11.3% in average. The extracted lignin is of powder state in brown, as seen in Fig. 4a. The particle sizes are not uniform and there are some particles aggregated. The aggregated particle size is in the range of 10–100 μm with different shapes. The lignin particles were uniformly pulverized to less than 10 μm in average size and then used for carbonization and activation.

The carbonized lignin with the yield of 40–43% was obtained from the extracted lignin by heat-treating at 600, 850, and 1000°C, respectively. Fig. 4 displays the visual appearance of the carbonized lignin before (b) and after (c) pulverization. As can be seen, the carbonized lignin was obtained in a bulky shape after carbonization process was performed with the extracted lignin powder. This is due probably to softening, melting and fusing together of the lignin particles occurring at around 250°C upon carbonization, as described above. After the pulverization,

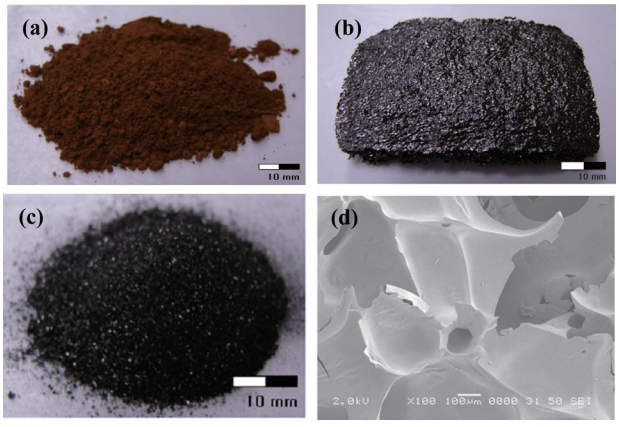

Fig. 4. Extracted lignin (a) and carbonized lignin samples (b-d): (b) before pulverization, (c) after pulverization, and (d) scanning electron microscope image of the sample pulverized after carbonized at 850°C (×100).

the carbonized lignin more or less looks shinier than the extracted lignin. Fig. 4d shows an SEM image of the lignin carbonized at 850°C. It is observed that the edges of the particle look sharp, showing a brittle pattern formed during the pulverization of the carbonized lignin.

3.3. Chemical composition

Table 2 lists the chemical compositions of the extracted lignin and the lignin carbonized at different temperatures. As expected, the carbon contents are considerably increased from about 60 to 88–94% with the carbonization temperature. On the other hand, the hydrogen and oxygen contents are decreased with the carbonization temperature as well. This is due to removal of hydrogen- and oxygen-containing components from the extracted lignin during the high temperature heat treatment process, being transformed to the carbonized structure. The result indicates that carbonization takes place rapidly in the early stage of the heat treatment process above 600°C, leading to a marked increase of the carbon assay.

3.4. Thermal stability of the extracted lignin and carbonized lignin

Fig. 5 shows the TGA curve (a) for the extracted lignin as a function of temperature. The initial weight loss of about 2–3% occurring near 100°C may be attributed to the removal of moisture remaining in the extracted lignin. The primary weight loss occurs beyond about 200°C. This may be explained by that around 250°C lignin can be softened, melted and then fused the lignin particles together, as reported earlier [39]. At this thermal stage, the guaiacyl or syringyl component is removed from the lignin and the chemical structure can be changed, resulting in some weight losses [40]. The small peak as shoulder at about 290°C in the derivative thermogravimetric analysis (DTG) curve (b) is due to removal of the hemicellulose component remaining in the lignin. Further weight losses occurring above 380°C may be due to degradation of the lignin with the phenol moiety [41]. The DTG curve indicates that the fastest weight loss occurs near 380°C. The residual weight at 800°C is about 34%.

Fig. 5 also shows TGA curves (c-e) measured with the lignin carbonized at different temperatures. The primary weight loss occurs near 550°C. The sample carbonized at 600°C exhibits the higher weight loss than the other two. It reflects that 600°C is not high enough to have the developed carbon structure for further heat treatment and the thermal stability is high enough. The thermal stability increases with increasing the carbonization temperature, as expected from the change of the carbon contents in Table 2. The difference in the residual weight measured at 800°C is smaller between the carbonization temperatures 850 and 1000°C than between 600 and 850°C. This is consistent with the result of the carbon content change described in Table 2. It turns out that the carbonized structure may be predominantly developed at above 850°C, resulting in the relatively high thermal stability.

Table 2. Chemical Compositions of the extracted lignin and carbonized lignin determined by elemental analysis

Lignin	Carbonization temperature	C (%)	H (%)	O (%)	N (%)
Extracted	No carbonization	60.4	5.6	33.8	0.2
Carbonized	600°C	88.4	2.5	8.5	0.6
	850°C	93.4	0.6	5.4	0.6
	1000°C	94.4	0.3	4.0	1.3

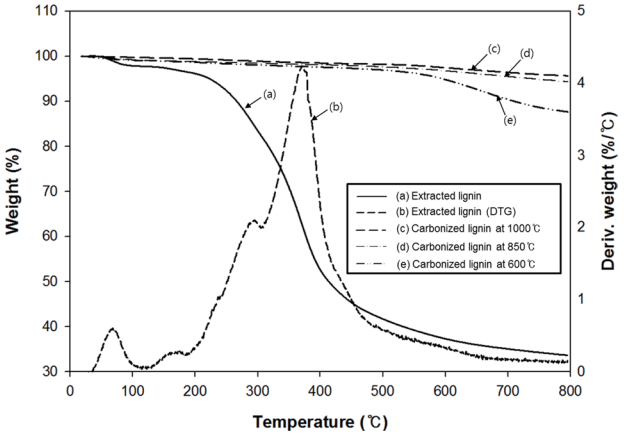

Fig. 5. Thermogravimetric analysis results measured for the extracted lignin (a), the derivative thermogravimetric analysis (DTG) curve (b), and the lignin samples carbonized at different temperatures: (c) 1000°C, (d) 850°C, and (e) 600°C. Deriv, derivative.

3.5. X-ray diffraction pattern of carbonized lignin

Fig. 6 represents the X-ray diffraction pattern of the lignin carbonized at different temperatures. With increasing the carbonization temperature, the peak intensity centered at 22° due to the (002) plane of graphite structure increases more or less, and the 2θ peak position at 22° shifts to the right slightly. As a result, it is expected that the ordered structure is not developed in the carbonized lignin yet, even though the slightly decreased spacing between the basal planes with increasing the carbonization

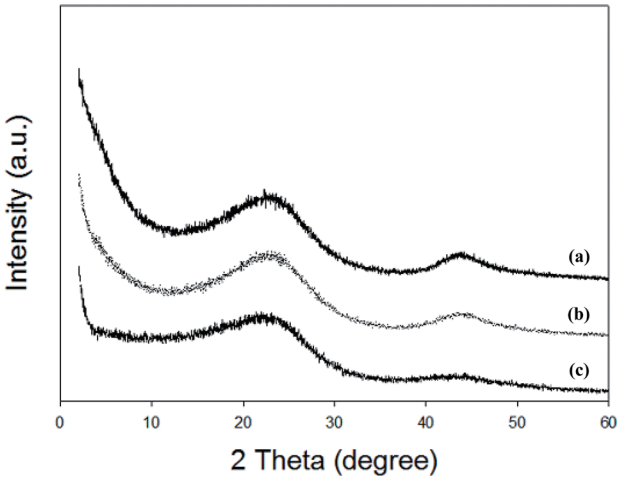

Fig. 6. X-ray diffraction curves measured for the lignin samples carbonized at different temperatures: (a) 1000°C, (b) 850°C, and (c) 600°C.

temperature is observed. The 2θ peak intensity at 43° due to the (100) plane increases with increasing the carbonization temperature. However, considering that there is no significant change in the peak intensity and position, it seems that the carbonized lignin obtained under the given heat treatment condition does not have well-developed microstructure, but it may be acceptable for activation.

3.6. Morphology and specific surface area

Fig. 7 represents SEM images observed from the surfaces of the lignin carbonized at 850°C (a and b) and the activated carbon (c and d) at different magnifications (×10,000, ×50,000). The carbonized lignin exhibits a smooth surface, which can be typically observed with brittle materials such as thermosetting polymers, reflecting the heat-treatment effect at high temperature. The activated carbon exhibits a rough surface with a large number of pores. It is obviously said that the pores are formed by the steam-activation process. That is, it is mentioned that the apparent surface area of the activated carbon is increased due to the thermo-oxidative reaction, being active in the presence of steam supplied during the activation process. During this steam activation process, carbon atoms existing in the surface of the carbonized lignin can be removed by water molecules in the supplied steam, evolving carbon monoxide and hydrogen gases [42]. A large number of pores including micropores are formed and the closed pores may also be transformed to the open pores. The formation of pores in the activated carbon results in the increase of specific surface area. Table 3 shows the specific surface area based on the microporous area and the external surface area, measured with the carbonized lignin and the activated carbon, respectively. The specific surface area value of the carbonized lignin is greatly increased from about 400 m^2/g to about 1720 m^2/g by the steam-activation process. About 59% of the total pore structure consists of the micropores. The result indicates that the steam-activation process plays a role in developing not only the microporous structure but also the externally porous structure besides the micropores.

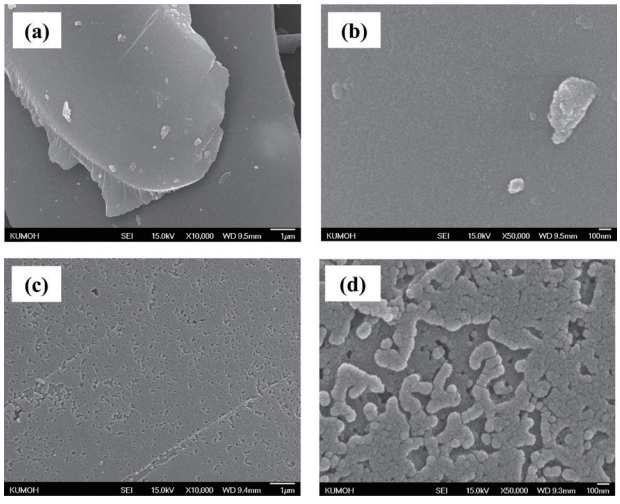

Fig. 7. Field emission-scanning electron microscope micrographs observed for (a, b) carbonized and (c, d) activated carbon samples (a, c: ×10,000; b, d: ×50,000).

Table 3. The specific surface areas measured for carbonized lignin and lignin-derived activated carbon

Lignin	Specific surface area (m^2/g)	Micropore area (m^2/g)	External surface area (m^2/g)
Carbonized	402	387	15
Activated	1718	1019	699

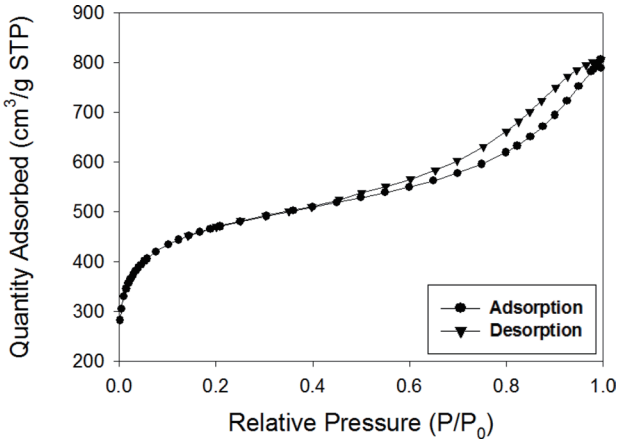

Fig. 8. Isotherm adsorption and desorption curves of the lignin-derived activated carbon.

Fig. 8 displays the isothermal adsorption-desorption curves as a function relative pressure obtained with the lignin-derived activated carbon by BET measurement. The absorption and desorption behavior, which is typically seen in highly porous materials, is found in the activated carbon. In the curve, there is some hysteresis, which can be often found in the solid sample consisting of aggregates, is due usually to a different behavior in adsorption and desorption [35]. Considering of the curve behavior, it may be mentioned that the pore size and shape in the activated carbon is somewhat uniform.

4. Conclusions

In the present study, biomass-based lignin was extracted from industrial waste black liquor and characterized to identify the lignin. The extracted lignin was carbonized and steam-activated to prepare biomass-derived activated carbon. The results reveal the feasibility of preparing the activated carbon with the following conclusions.

The lignin extracted from 'as-supplied' black liquor exhibits typical characteristic infrared absorption peaks and chemical shift values of lignin. The carbon residue at 800°C of the extracted lignin is about 34%, which is somewhat affordable for carbonization. The carbonized lignin shows a brittle surface topography, the increased thermal stability, and the carbon assay with increasing the carbonization temperature. The activated carbon prepared from the extracted lignin via carbonization and steam-activation processes exhibits well-developed pore struc-

ture including the micropores dominantly. The SEM images and the BET result elucidate that the activated carbon has the specific surface area about 4.3 times greater than the carbonized lignin, giving the value of 1718 m^2/g.

Conflict of Interest

No potential conflict of interest relevant to this article was reported.

Acknowledgements

This research was supported by Nuclear R&D Program (NRF-2015M2A2A6A03044942) through the National Research Foundation funded by the Ministry of Science, ICT and Future Planning, Korea.

References

[1] *Biermann CJ. Essentials of Pulping and Papermaking, Academic Press, San Diego (1993).*

[2] Sricharoenchaikul V, Hicks AL, Frederick WJ. Carbon and char residue yields from rapid pyrolysis of kraft black liquor. Bioresour Technol, **77**, 131 (2001). https://doi.org/10.1016/s0960-8524(00)00155-3.

[3] Demirbaş A. Pyrolysis and steam gasification processes of black liquor. Energy Convers Manage, **43**, 877 (2002). https://doi.org/10.1016/s0196-8904(01)00087-5.

[4] Cheng H, Zhan H, Fu S, Lucia LA. Alkali extraction of hemicellulose from depithed corn stover and effects on soda-aq pulping. Bioresources, **6**, 196 (2011).

[5] Cardoso M, de Oliveira ED, Passos ML. Chemical composition and physical properties of black liquors and their effects on liquor recovery operation in Brazilian pulp mills. Fuel, **88**, 756 (2009). https://doi.org/10.1016/j.fuel.2008.10.016.

[6] Ibrahim MM, Agblevor FA, EL-Zawawy WK. Isolation and characterization of cellulose and lignin from steam-exploded lignocellulosic biomass. Bioresources, **5**, 397 (2010).

[7] Goujon T, Ferret V, Mila I, Pollet B, Ruel K, Burlat V, Joseleau JP, Barrière Y, Lapierre C, Jouanin L. Down-regulation of the AtCCR1 gene in Arabidopsis thaliana: effects on phenotype, lignins and cell wall degradability. Planta, **217**, 218 (2003).

[8] Fox C. Chemical and Thermal Characterization of Three Industrial Lignins and Their Corresponding Lignin Esters, University of Idaho, Moscow, ID, MS Thesis (2006).

[9] García A, Toledano A, Serrano L, Egüés I, González M, Marín F, Labidi J. Characterization of lignins obtained by selective precipitation. Sep Purif Technol, **68**, 193 (2009). http://doi.org/10.1016/j.seppur.2009.05.001.

[10] Bhat R, Khalil HPSA, Karim AA. Exploring the antioxidant potential of lignin isolated from black liquor of oil palm waste. C R Biol, **332**, 827 (2009). https://doi.org/10.1016/j.crvi.2009.05.004.

[11] Mussatto SI, Fernandes M, Roberto IC. Lignin recovery from brewer's spent grain black liquor. Carbohydr Polym, **70**, 218 (2007). https://doi.org/10.1016/j.carbpol.2007.03.021.

[12] Rohella RS, Sahoo N, Paul SC, Choudhury S, Chakravortty V. Thermal studies on isolated and purified lignin. Thermochim Acta, **287**, 131 (1996). https://doi.org/10.1016/0040-6031(96)02983-8.

[13] Kim YS, Kadla JF. Preparation of a thermoresponsive lignin-based biomaterial through atom transfer radical polymerization. Biomacromolecules, **11**, 981 (2010). https://doi.org/10.1021/bm901455p.

[14] Vanholme R, Demedts B, Morreel K, Ralph J, Boerjan W. Lignin biosynthesis and structure. Plant Physiol, **153**, 895 (2010). https://dx.doi.org/10.1104/pp.110.155119.

[15] Takayama M, Johjima T, Yamanaka T, Wariishi H, Tanaka H. Fourier transform Raman assignment of guaiacyl and syringyl marker bands for lignin determination. Spectrochim Acta Part A, **53**, 1621 (1997). https://doi.org/10.1016/s1386-1425(97)00100-5.

[16] Wu X, Gallego NC, Contescu CI, Tekinalp H, Bhat VV, Baker FS, Thies MC. The effect of processing conditions on microstructure of Pd-containing activated carbon fibers. Carbon, **46**, 54 (2008). https://doi.org/10.1016/j.carbon.2007.10.036.

[17] Kim JM, Song IS, Cho DH, Hong IP. Effect of carbonization temperature and chemical pre-treatment on the thermal change and fiber morphology of kenaf-based carbon fibers. Carbon Lett, **12**, 131 (2011). https://doi.org/10.5714/cl.2011.12.3.131.

[18] Lee HM, An KH, Kim BJ. Effects of carbonization temperature on pore development in polyacrylonitrile-based activated carbon nanofibers. Carbon Lett, **15**, 146 (2014). https://doi.org/10.5714/cl.2014.15.2.146.

[19] Karagöz S, Tay T, Ucar S, Erdem M. Activated carbons from waste biomass by sulfuric acid activation and their use on methylene blue adsorption. Bioresour Technol, **99**, 6214 (2008). https://doi.org/10.1016/j.biortech.2007.12.019.

[20] Tancredi N, Cordero T, Rodríguez-Mirasol J, Rodríguez JJ. Activated carbons from uruguayan eucalyptus wood. Fuel, **75**, 1701 (1996). https://doi.org/10.1016/s0016-2361(96)00168-8.

[21] Huang DC, Liu QL, Zhang W, Ding J, Gu JJ, Zhu SM, Guo QX, Zhang D. Preparation of high-surface-area activated carbon from zizania latifolia leaves by one-step activation with K_2CO_3/rarefied air. J Mater Sci, **46**, 5064 (2011). https://doi.org/10.1007/s10853-011-5429-4.

[22] Jang JS, Lee YS, Kim IK, Yim G. Chemical activation characteristics of pitch-based carbon fibers by KOH. Carbon Lett, **1**, 69 (2000).

[23] Mui ELK, Ko DCK, McKay G. Production of active carbons from waste tyres: a review. Carbon, **42**, 2789 (2004). https://doi.org/10.1016/j.carbon.2004.06.023.

[24] Yang SC, Lee YS, Kim JH, Lim CK, Park YT. Preparation and properties of pelletized activated carbons using coconut char and coal-tar pitch. Carbon Lett, **2**, 176 (2001).

[25] Lee E, Kwon SH, Choi PR, Jung JC, Kim MS. Activated carbons prepared from mixtures of coal tar pitch and petroleum pitch and their electrochemical performance as electrode materials for electric double-layer capacitor. Carbon Lett, **16**, 78 (2015). https://doi.org/10.5714/cl.2015.16.2.078.

[26] Hill TL. Adsorption from a one-dimensional lattice gas and the Brunauer-Emmett-Teller equation. Proc Natl Acad Sci USA, **93**, 14328 (1996). https://doi.org/10.1073/pnas.93.25.14328.

[27] Moon DJ, Chung MJ, Kim H, Lee BG, Lee SD, Park KY. Adsorption equilibria of chloropentafluoroethane on activated carbon powder. Korean J Chem Eng, **15**, 619 (1998). https://doi.org/10.1007/bf02698988.

[28] Harding AW, Foley NJ, Norman PR, Francis DC, Thomas KM. Diffusion barriers in the kinetics of water vapor adsorption/desorp-

tion on activated carbons. Langmuir, **14**, 3858 (1998). https://doi.org/10.1021/la971317o.

[29] Ronga H, Ryua Z, Zhenga J, Zhangb Y. Effect of air oxidation of rayon-based activated carbon fibers on the adsorption behavior for formaldehyde. Carbon, **40**, 2291 (2002). https://doi.org/10.1016/s0008-6223(02)00109-4.

[30] Czepirski L, Balys MR, Komorowska-Czepirska E. Some generalization of Langmuir adsorption isotherm. Internet J Chem, **3**, 14 (2000).

[31] Cho D, Kim JM, Song IS, Hong I. Effect of alkali pre-treatment of jute on the formation of jute-based carbon fibers. Mater Lett, **65**, 1492 (2011). https://doi.org/10.1016/j.matlet.2011.02.050.

[32] Phan NH, Rio S, Faur C, Coq LL, Cloirec PL, Nguyen TH. Production of fibrous activated carbons from natural cellulose (jute, coconut) fibers for water treatment applications. Carbon, **44**, 2569 (2006). https://doi.org/10.1016/j.carbon.2006.05.048.

[33] Manocha S, Chauhan VB, Manocha LM. Porosity development on activation of char from dry and wet babbool wood. Carbon Sci, **3**, 133 (2002).

[34] Hong I, Kim KH, Park SM, Lee SY, Park H. Preparation of pulp waste based adsorbents and their properties. Proceedings of Annual World Conference on Carbon 2010, Clemson, SC, 670 (2010).

[35] Leofanti G, Padovan M, Tozzola G, Venturelli B. Surface area and pore texture of catalysts. Catal Today, **41**, 207 (1998). https://doi.org/10.1016/S0920-5861(98)00050-9.

[36] Bykov I. Characterization of Natural and Technical Lignins Using FTIR Spectroscopy, Lulea University of Technology, Lulea, MS Thesis (2008).

[37] Higuchi T. Biochemistry of wood components: biosynthesis and microbial degradation of lignin. Wood Res Bull Wood Res Inst Kyoto Univ, **89**, 43 (2002).

[38] Toledano A, Serrano L, Garcia A, Mondragon I, Labidi J. Comparative study of lignin fractionation by ultrafiltration and selective precipitation. Chem Eng J, **157**, 93 (2010). https://doi.org/10.1016/j.cej.2009.10.056.

[39] Baliga V, Sharma R, Miser D, McGrath T, Hajaligol M. Physical characterization of pyrolyzed tobacco and tobacco components. J Anal Appl Pyrolysis, **66**, 191 (2003). https://doi.org/10.1016/S0165-2370(02)00114-6.

[40] Brodin I, Sjöholm E, Gellerstedt G. The behavior of kraft lignin during thermal treatment. J Anal Appl Pyrolysis, **87**, 70 (2010). https://doi.org/10.1016/j.jaap.2009.10.005.

[41] Haykiri-Acma H, Yaman S, Kucukbayrak S. Comparison of the thermal reactivities of isolated lignin and holocellulose during pyrolysis. Fuel Process Technol, **91**, 759 (2010). https://doi.org/10.1016/j.fuproc.2010.02.009.

[42] Kim D. Preparation and Characterization of Renewable Biomass-based Activated Carbon from Lignin and Lignin/Phenolic Composite Resins, Kumoh National Institute of Technology, Gumi, MS Thesis (2011).